Postnatal Expansion, Maturation and Functionality of MR1T Cells in Humans

Gwendolyn M. Swarbrick[1,4¶*], Anele Gela[5¶], Meghan E. Cansler[1], Megan D. Null[1], Rowan B. Duncan[1], Elisa Nemes[5], Muki Shey[5, 6], Mary Nsereko[7], Harriet Mayanja-Kizza[7, 8], Sarah Kiguli[7, 9], Jeffrey Koh[3], Willem A. Hanekom[5], Mark Hatherill[5], Christina Lancioni[1], David M. Lewinsohn[2, 4], Thomas J. Scriba[5&], Deborah A. Lewinsohn[1&]

[1]Division of Infectious Diseases, Department of Pediatrics, Oregon Health & Science University, Portland, Oregon, USA

[2]Division of Pulmonary and Critical Care Medicine, Department of Medicine, Oregon Health & Science University, Portland, Oregon, USA

[3]Department of Anesthesiology and Perioperative Medicine, Oregon Health & Science University, Portland, Oregon, USA

[4]Portland Veterans Administration Healthcare System, Portland, Oregon, USA

[5]South African Tuberculosis Vaccine Initiative, Institute of Infectious Disease and Molecular Medicine and Division of Immunology, Department of Pathology, University of Cape Town, Cape Town, South Africa

[6]Department of Medicine & Wellcome Centre for Infectious Disease Research in Africa (CIDRI-Africa), Institute of Infectious Disease and Molecular Medicine, University of Cape Town, South Africa

[7]Uganda-CWRU Research Collaboration, Kampala, Uganda.

[8]Dept of Medicine, Makerere University, Kampala, Uganda.

[9]Dept of Paediatrics, Makerere University, Kampala, Uganda.

*Correspondence
Gwendolyn Swarbrick
swarbric@ohsu.edu

¶These authors contributed equally to this work.

&These authors are Joint Senior Authors.

Keywords: innate T cells, human mucosal immunology, MAIT cells, infant, tuberculosis.

Abstract

MR1-restricted T (MR1T) cells are defined by their recognition of metabolite antigens presented by the monomorphic MHC class 1-related molecule, MR1, the most highly conserved MHC class I related molecule in mammalian species. Mucosal-associated invariant T (MAIT) cells are the predominant subset of MR1T cells expressing TRAV1-2. These cells comprise a T cell subset that recognizes and mediates host immune responses to a broad array of microbial pathogens, including *Mycobacterium tuberculosis*. Here, we sought to characterize development of circulating human MR1T cells defined by MR1-5-OP-RU tetramer labelling and of the MAIT cell subset, defined by expression of TRAV1-2 and high expression of CD26 and CD161 (TRAV1-2^{+}CD161^{++}CD26^{++} cells). We analysed postnatal expansion, maturation and functionality of peripheral blood MR1T cells in cohorts from three different geographic settings with different tuberculosis (TB) vaccination practices, levels of exposure to and infection with *M. tuberculosis.* Early after birth, frequencies of MR1-5-OP-RU tetramer-defined MR1T cells increased rapidly by several fold. This coincided with the transition from a predominantly CD4^{+} and TRAV1-2^{-} population in neonates, to a predominantly TRAV1-2^{+}CD161^{++}CD26^{++} CD8^{+} population. We also observed that tetramer^{+} MR1T cells that expressed TNF upon mycobacterial stimulation were very low in neonates, but increased ~10-fold in the first year of life. These functional MR1T cells in all age groups were MR1-5-OP-RU tetramer^{+}TRAV1-2^{+} and highly expressed CD161 and CD26, markers that appeared to signal phenotypic and functional maturation of this cell subset. This age-associated maturation was also marked by the loss of naïve T cell markers on tetramer^{+} TRAV1-2^{+} MR1T cells more rapidly than tetramer^{+}TRAV1-2^{-} MR1T cells and non-MR1T cells. These data suggest that neonates have infrequent populations of MR1T cells with diverse phenotypic attributes; and that exposure to the environment rapidly and preferentially expands the MR1-5-OP-RU tetramer^{+}TRAV1-2^{+} population of MR1T cells, which becomes the predominant population of functional MR1T cells early during childhood.

Introduction

MR1-restricted T (MR1T) cells and mucosal-associated invariant T (MAIT) cells, which are the predominant subset of MR1T cells expressing TRAV1-2, are T-cells that display a highly restricted T-cell-receptor (TCR) repertoire and exhibit innate-like functions similar to those described for NKT cells. MR1T cells are defined by their recognition of metabolite antigens presented by the monomorphic MHC class 1-related molecule, MR1, the most highly conserved MHC class I related molecule in mammalian species (Harriff et al., 2018; Godfrey et al., 2019). The TRAV1-2^{+} MAIT cell subset express an invariant TCR α-chain (TRAV1.2-TRAJ33/20/12 in humans; TRAV1-TRAJ33 in mice) with a CDR3 of constant length paired with a limited number of Vβ segments (Vβ2/13 in humans; Vβ6/8 in mice) (Treiner et al., 2003; Martin et al., 2009; Reantragoon et al., 2013; Lepore et al., 2014). MR1T cells have been defined by different methods. Prior to availability of the MR1 tetramer, MR1T cells were phenotypically defined as the predominant MAIT cell subset, by expression of TRAV1-2 and high level expression of CD161 (Walker et al., 2012; Fergusson et al., 2014; Sharma et al., 2015) and CD26 (Sharma et al., 2015). Now the MR1 tetramer can also be more broadly used to define MR1T cells. In peripheral blood, MAIT cells defined by MR1 tetramer or phenotype are highly concordant in adults (Meermeier et al., 2016). As we will show in this paper, the MR1 tetramer allows detection of a much broader repertoire of MR1Ts that are not only restricted to TRAV1-2^{+} (MAIT cells).

MR1T cell development is a stepwise process, with an intra-thymic selection followed by peripheral expansion. Using the MR1 tetramer, Koay *et al* reported a three-stage development pathway for mouse and human MR1T cell populations, where three populations of human MR1T precursors were defined based on differential expression of CD27 and CD161. The initial two stages of MR1-5-OP-RU tetramer^{+}TRAV1-2^{+}CD161^{-} cells, which were either CD27^{-} or CD27^{+}, occurred in the thymus and these cells were low in the periphery. The more mature MR1 tetramer^{+}TRAV1-2^{+}CD161^{+}CD27^{+} cells, designated as stage 3, have been shown to represent only a small fraction of T cells in the thymus and neonates but form a more abundant population in adult blood (Martin et al., 2009; Dusseaux et al., 2011; Koay et al., 2016). Studies utilizing TRAV1-2 and high level CD161 expression (CD8^{+}TRAV1-2^{+}CD161^{++} cells) to define MAIT cells, similarly demonstrated low numbers of these cells in the neonates, which expand postnatally (Walker et al., 2012; Fergusson et al., 2014). Such studies indicate that MR1T cell thymopoeisis is complemented by an important postnatal peripheral expansion and maturation, which was recently shown to be dependent upon acquisition of the intestinal microbiome (Constantinides et al., 2019; Legoux et al., 2019).

MR1T cells are activated via both TCR-dependent and TCR-independent mechanisms. Regarding TCR-dependent activation, MR1T cells recognize microbial derived riboflavin (Vitamin B2) biosynthesis intermediate derivatives, such as 5-OP-RU (5-(2-oxopropylideneamino)-6-d-ribitylaminouracil) and a broad spectrum of microbes that synthesize riboflavin, including *S. aureus, E. coli, and C. albicans* (Gold et al., 2010; Kjer-Nielsen et al., 2012; Gold et al., 2013; Corbett et al., 2014; Meermeier et al., 2016). While 5-OP-RU was the first activating MR1 ligand defined, several other ligands have subsequently been defined, including additional riboflavin-derived ligands, and both stimulatory and inhibitory ligands (Eckle et al., 2014; Gherardin et al., 2016; Meermeier et al., 2016; Harriff et al., 2018). In addition, cytokines,

primarily IL-12, IL-18, and IL-15, act synergistically to activate MR1T cells, both by lowering the threshold of TCR activation (Ussher et al., 2014; Sattler et al., 2015; Slichter et al., 2016) and/or inducing MR1-independent activation (Fergusson et al., 2014; Ussher et al., 2014; Sattler et al., 2015; Slichter et al., 2016; van Wilgenburg et al., 2016; Suliman et al., 2020). These TCR-independent activation mechanisms are hypothesized to explain how MR1T cells may participate in host defense to viruses and bacteria that do not synthesize riboflavin (Ussher et al., 2014; van Wilgenburg et al., 2016). Once activated, MR1T cells display immediate effector function by secreting inflammatory cytokines and cytotoxic molecules, which can kill infected cells (Gold et al., 2010; Dusseaux et al., 2011; Le Bourhis et al., 2013; Kurioka et al., 2015). In a mouse model of pulmonary legionella infection, MR1T cells afforded enhanced protection in an MR1-dependent manner, mediated by the effector molecules IFN-γ and GM-CSF (Wang et al., 2018). MR1T cells have also been shown to facilitate control of *Klebsiella pneumoniae, Mycobacterium bovis* BCG, and *Francicella tularensis* infections (Georgel et al., 2011; Meierovics et al., 2013; Sakala et al., 2015; Meierovics and Cowley, 2016). Many of the bacterial pathogens that are important causes of infant morbidity and mortality, including *S. aureus*, *S. pneumoniae*, and enteric pathogens (e.g. *E. coli*, *Klebsiella*, *Salmonella*), are recognized by MR1T cells. Moreover, MR1T cells may contribute to viral immunity and hence host defense to viral pneumonia, which represents the major cause of morbidity and mortality worldwide (Zar and Ferkol, 2014). MR1T cells possess immediate innate-like, effector functions, and can therefore mediate immune functions before priming, clonal expansion and maturation of antigen-specific MHC-restricted T cells (Gold et al., 2013; Hartmann et al., 2018; Godfrey et al., 2019). Therefore, MR1T cells could play an important role in host defense to a variety of pathogens, especially in infancy.

MR1T cells are known to also recognize and respond to *Mycobacterium tuberculosis,* the leading global cause of mortality from a single infectious agent. Infants and young children suffer disproportionately from disseminated and severe forms of tuberculosis (TB) disease and are significantly more susceptible to disease than adults (Marais et al., 2004a; Marais et al., 2004b; Marais et al., 2006). Here, we sought to characterize development of MR1T cells (defined by MR1-tetramer labeling) and their subset of phenotypically defined MAIT cells (TRAV1-2^{+}CD161^{++}CD26^{++} T cells) by analyzing postnatal expansion, maturation and functionality in humans. We compared MR1T/MAIT cell development in cohorts from three different settings with differing TB vaccination practices and levels of exposure and infection with *M. tuberculosis.*

Results

Human participants

We enrolled nine cohorts across three different countries to study MR1T cell development (Table 1). The cohorts in South Africa (SA) were neonates (cord blood, *n* = 10), infants (aged 10 weeks, BCG vaccinated at birth, *n* = 10) and adolescents [aged 14-18 years, BCG vaccinated at birth, QuantiFERON-TB Gold (QFT)-negative, *n* = 10]. The cohorts enrolled in the United States (US) were neonates (cord blood, *n* = 10), infants (aged 9-15 months, BCG unvaccinated, *n* = 10) and adults (aged 29-60 years, *n* = 10). The cohorts in Uganda (UG) were infants [2-24 months old, BCG vaccinated at birth +/-, tuberculin skin test (TST) +/-, *n* = 36], children (24 - 60 months, BCG vaccinated at birth +/-, TST +/-, *n* = 23) and adults (aged 18-60 years, BCG vaccinated at birth +/-, TST +/-, *n* = 91).

Frequencies of tetramer-defined MR1T cell and phenotypically defined MAIT cell populations increase with age irrespective of BCG vaccination

We defined MR1T cells as $CD3^+$ T cells positively labeled with the MR1-5-OP-RU tetramer. The MR1-6FP tetramer was as a negative control tetramer (Figure 1A). The MR1-6-FP tetramer stained a different population of cells than the MR1-5-OP-RU tetramer (Figure S1). The MR1T cell subset, MAIT cells, were defined phenotypically as $CD3^+$ T cells that co-expressed TRAV1-2 and high levels of CD161 ($CD161^{++}$) and CD26 ($CD26^{++}$) (Figure 1A and Figure S2). This phenotypic definition of MAIT cells is concordant with the vast majority of tetramer-defined MR1T cells in adults (Sharma et al., 2015; Meermeier et al., 2016). We determined frequencies of MR1T cells and the phenotypically-defined MAIT cell subset in all cohorts (Figure 1B). Because of limited availability of the MR1-5-OP-RU tetramer, determination of tetramer-defined MR1T cell frequencies in the Ugandan cohorts was performed on a subset of 10 donors (Figure 1B and Figure S3). In all cohorts, both tetramer-defined MR1T cell and phenotypically-defined MAIT cell frequencies (Figure 1B) and absolute cell numbers (Figure S4) increased with age.

Tetramer-defined MR1T cell and phenotypically-defined MAIT cell populations are concordant in adults, adolescents and infants but discordant in neonates

We next determined the degree of concordance between tetramer-defined MR1T cell and phenotypically-defined MAIT cell populations. The majority of the phenotypically-defined MAIT cell population (TRAV1-$2^+$$CD161^{++}$$CD26^{++}$ cells) also stained with the MR1 tetramer in infants, adolescents and adults, demonstrating high concordance between tetramer-defined MR1T cells and phenotypically-defined MAIT cells in these cohorts. (Figure 1C). However, in cord blood from both SA and US neonates, these two populations were discordant as the minority of TRAV1-2^+ $CD161^{++}$$CD26^{++}$ MAIT cells also stained with the MR1T tetramer (Figure 1C).

The MR1-5-OP-RU tetramer$^+$ subset of phenotypically-defined MAIT cells contain the functional population

To investigate whether tetramer-defined MR1T cells and phenotypically-defined MAIT cells have different functional capacity, we measured TNF expression in the US cohort by intracellular cytokine staining (ICS) and flow cytometry following incubation with *M. smegmatis*-infected A549 cells. Among all phenotypically defined TRAV1-$2^+$$CD161^{++}$$CD26^{++}$ MAIT cells, only the MR1-5-OP-RU tetramer$^+$ subset expressed TNF; MR1-5-OP-RU tetramer-negative cells,

166 by contrast, did not appear to respond to *M. smegmatis* stimulation (Figure 2). Because of this
167 result, we focused on the functional, tetramer-defined ($CD3^+$MR1-5-OP/RU^+) MR1T cells for
168 subsequent experiments.

169 **Neonates have higher proportions of $CD4^+$ and TRAV1-2^- MR1T populations compared to**
170 **infants, adolescents and adults**

171 To explore the diversity of MR1T cells and how this may change during early development,
172 we applied the dimensionality reduction method, t-distributed stochastic neighbor embedding
173 (tSNE), on tetramer-defined MR1T cells. Five discrete phenotypic MR1T cell clusters were
174 identified in both the SA and US cohorts (Figure 3A-D), the relative proportions of which varied
175 with age (Figure 3B and D). Specifically, the $CD4^+$ (Clusters 3 and 4) and TRAV1-$2^-$$CD26^-$
176 $CD161^-$ (Clusters 1, 2 and 3) MR1T cell clusters predominated in neonates, while $CD4^-CD8^{+/-}$
177 TRAV1-$2^+CD26^+CD161^+$ cluster (Cluster 5) was predominant in infant, adolescent, and adult
178 cohorts from both the US and SA (Figure 3B and D). Relative proportions of MR1T cell clusters
179 in 10 week old (SA) and 12 month old (US) infants were more similar to those in adults and
180 adolescents than to those in neonates, consistent with the hypothesis that MR1T cells mature
181 rapidly upon exposure to MR1T cell antigens (Figure 3E and F). It was also noteworthy that $CD4^-$
182 $CD8^{+/-}$TRAV1-$2^+CD161^+CD26^+$ MR1T cells that fell into cluster 5 comprised a much lower
183 percentage of the MR1Ts in cord blood, while forming the dominant phenotype in 12-month-old
184 (US) infants. In the 10 week old (SA) infants, this cluster had started to appear but was not yet
185 "fully developed", suggesting rapid development during the first months of life, from a
186 predominantly TRAV1-2 negative to a TRAV1-2 positive population with loss of expression of
187 CD4 and acquisition of CD26 and CD161. We also note that in the US cohort only there is a
188 population that is positive for all markers (Cluster 6) that is present at low frequency in all ages.

189 **MR1T cells become more functional with age**

190 Next, we explored how tetramer-defined MR1T cells developed functionally with age in
191 the US cohort by tracking the TNF-expressing population following *M. smegmatis* or
192 PMA/Ionomycin stimulation. TNF-expressing $tetramer^+$ MR1T cells in neonates were present at
193 very low frequencies (Figure 2B) and represented a much smaller proportion of the total $tetramer^+$
194 MR1T cell population than in infants and adults (Figure 4A and B). Proportions of $tetramer^+$ MR1T
195 cells responding to either mycobacteria or PMA/Ionomycin were higher in infants than adults
196 ($p=0.0007$ and $p=0.0021$, respectively) or neonates ($p<0.0001$ for both stimulations). However,
197 because $tetramer^+$ MR1T cell frequencies were higher in adults than infants (Figure 1B), overall
198 frequencies of TNF-producing MR1T cells were highest in adults. To explore the functional
199 capacity of MR1T cells relative to other T cell subsets within each cohort, we compared
200 proportions of TNF-expressing MR1T cells ($CD3^+TCR\gamma\delta^-$MR1-5-OP-RU^+) with TCRγδ T cells
201 ($CD3^+TCR\gamma\delta^+$ MR1-5OPRU^-), $CD4^+$ T cells ($CD3^+TCR\gamma\delta^-$MR1-5OPRU^-CD4^+) and $CD8^+$ T cells
202 ($CD3^+TCR\gamma\delta^-$MR1-5OPRU^-CD4^+) after PMA/Ionomycin stimulation (Figure 4C). In neonates,
203 proportions of TNF-expressing MR1T cells were significantly higher than proportions of TCRγδ
204 T cells and $CD8^+$ T cells. In infants and adults, proportions of TNF-expressing MR1T cells were
205 significantly higher than $TCR\gamma\delta^+$, $CD4^+$ and $CD8^+$ T cells (Figure 4C).

206 **Functional CD3$^+$MR1-5-OP-RU$^+$ MR1T cells are TRAV1-2$^+$**

207 Next, we investigated TRAV1-2 expression among functional, TNF-expressing
208 CD3$^+$MR1-5-OP-RU$^+$ MR1T cells. Only TRAV1-2$^+$ MR1T cells produced TNF in response to
209 mycobacterial stimulation while TRAV1-2$^-$ MR1T cells were not functional (Figure 4D). This
210 pattern was unique to mycobacterial stimulation since TNF-expressing TRAV1-2$^-$ MR1T cells
211 were observed in response to PMA/Ionomycin stimulation, particularly in infants and adults
212 (Figure 4E). Interestingly, the vast majority of these functional, TNF-expressing TRAV1-2$^+$
213 MR1T cells also highly expressed the phenotypic markers, CD26 and CD161 (Figure 4F-G). Thus,
214 the CD3$^+$MR1-5-OP-RU$^+$TRAV1-2$^+$CD161^{++}CD26^{++} MR1T cell population contains the
215 functional MR1T cells that respond to mycobacteria. The frequency of this population increases
216 very quickly with age.

217 **TRAV1-2$^+$ MR1T cells lose naïve markers more rapidly with age than TRAV1-2$^-$ MR1T cells**
218 **or non-MR1T cells**

219 To characterize the development of MR1T cells further, we also measured expression of
220 CD27 and CD161, markers previously described to indicate MR1T cell maturation (Koay et al.,
221 2018), and CD45RA, CCR7, CD38 and CD56 on tetramer-defined MR1Ts (Figures 5-6). A
222 population of immature MR1T cells, defined as CD27$^+$CD161$^-$ cells, was observed in neonates but
223 not in infants and adults, as previously described (Koay et al., 2016). This was also reflected by
224 expression of the more traditional T cell maturation markers, CD45RA, CCR7 and CD38 (Figure
225 6 A, C, E). Most tetramer-defined MR1T cells in neonates displayed a CD45RA$^+$CCR7$^+$CD38$^+$
226 "naïve" phenotype, but this phenotype was lost more rapidly with age on TRAV1-2$^+$ MR1T cells
227 than on TRAV1-2$^-$ MR1T cells or non-MR1T cells (Figure 6A-F). The inverse was true for the
228 activation marker, CD56, which was increased in neonatal, infant and adult TRAV1-2$^+$ tetramer-
229 defined MR1T cells compared to TRAV1-2$^-$ tetramer-defined MR1T cells and non-MR1T cells
230 (Figure 6G-H). These results are consistent with our finding that TRAV1-2$^+$ tetramer-defined
231 MR1T cells display functional capacity in all age groups, even though they represent the minority
232 of neonatal MR1T cells.

233 **Discussion**

234 We characterized the development of MR1T cells during early childhood in three cohorts,
235 two from Africa and one in the USA, to elucidate phenotypic and functional changes that occur
236 after birth and during the first few years of life. A better understanding of MR1T cell development
237 is critical given the likely role of MR1T cells as innate-like effectors that act as key mediators of
238 immunity in newborns, who are at very high risk of infection, including *M. tuberculosis.* We found
239 that neonates had relatively low frequencies of MR1T cells with high phenotypic diversity, which
240 included considerable proportions of $CD4^+$ and TRAV1-2^- cells. These patterns changed as early
241 as 10 weeks after birth, and became more prominent at 1-2 years of age, adolescence and ultimately
242 by adulthood. This included higher frequencies of MR1T cells in peripheral blood, characterized
243 by a preferential expansion in TRAV1-2^+CD8^+ MR1T cells such that TRAV1-2^+CD8^+MR1T cells
244 constituted the vast majority of the $tetramer^+$ MR1T cell population. The development also
245 included changes in expression of maturation markers and MR1T cell effector function, since
246 MR1T cells from older individuals had lower expression of the naïve T cell markers, CD45RA,
247 CCR7 and CD38, and an increased ability to express TNF.

248 Our finding that MR1T cells are found at low frequency in cord blood and increase in
249 frequency with age confirms our previous observations, as well as those of others, who have
250 utilized either the MR1-5-OP-RU tetramer or phenotypic characterization of MAIT cells to
251 demonstrate the expansion of these cell populations from birth through adulthood (Martin et al.,
252 2009; Walker et al., 2012; Gold et al., 2013; Walker et al., 2014; Koay et al., 2016; Ben Youssef
253 et al., 2018; Gherardin et al., 2018). The very rapid changes in MR1T cells seen after birth are
254 striking and were clearly seen in both African and American settings. This finding rules out the
255 possibility that BCG substantially contributes to these changes, since BCG is not routinely
256 administered at birth in the USA and is consistent with the lack of differences in MAIT cell
257 magnitude or function between young infants either BCG immunized or unimmunized (Suliman
258 et al., 2020). Rather, it is more likely that changes occur upon the transition from the limited
259 microbial exposure in the womb to the postnatal environment, accompanied by the rapid
260 colonization of the gut microbiome. MR1T cells are absent in germ-free mice and depend on the
261 colonization of the gut microbiome with normal intestinal flora, which produce riboflavin (Le
262 Bourhis et al., 2013; Harriff et al., 2018; Legoux et al., 2019). We suggest that this colonization of
263 the gut microbiome is the driving force that accounts for the increase and phenotypic changes in
264 MR1T cells in blood after birth and the gain in functional capacity.

265 While we confirm our previous work that phenotypic definition of MAIT cells accurately
266 identifies functional MR1T cells in adults, we find that there is a high level of discordance in
267 neonates in part due to MR1-5-OP-RU $tetramer^+$ cells that do not express TRAV1-2, and/or high
268 levels of CD161 or CD26. These cells are by definition MR1-restricted T cells as they bind the
269 MR1-5-OP-RU tetramer. However, these cells are poorly reactive to mycobacteria, suggesting
270 that they either recognize a different antigen or represent immature MR1T cells. The poor
271 PMA/Ionomycin-induced TNF secretion of these cells supports the latter. However, because our
272 only measure of MR1T cell responses was TNF production, we may have failed to detect other
273 responses characterized by the production of alternative cytokines or cytolytic markers.

We also show that neonates possess MR1-5-OP-RU tetramer$^-$ cells that phenotypically resemble MAIT cells (the discordant MR1-5-OP-RU tetramer$^-$ phenotypically defined TRAV1-2$^+$CD161^{++}CD26^{++} MAIT cell population). As Fergusson *et al* suggested that distinct T subsets that express CD161 share a common transcriptional profile characteristic of typical MR1T cells (Fergusson et al., 2014), it is certainly possible that these CD161^{++} cells are MR1-restricted or share common attributes with MR1T cells. Further characterization of this neonatal T cell population is required to determine whether or not these cells are indeed MR1-restricted and if so, if these cells are immature or recognize distinct microbes, or produce a different cytokine not detected in our functional assay. Given that, in the mouse model, 5-OP-RU produced by the microbiome is necessary and sufficient to drive the expansion of typical MR1T cells (Legoux et al., 2019), it is perhaps expected that with age tetramer-positive MR1T TRAV1-2$^+$ cells would quickly become the predominant MR1T cell population, while tetramer negative MR1T cells might persist as a minority population of naïve T cells.

Consistent with our prior findings (Gold et al., 2013) and those of others (Walker et al., 2012; Ben Youssef et al., 2018), our phenotypic analysis of MR1-5-OP-RU tetramer$^+$ cells in neonates demonstrates that MR1T cells expressed a naïve cell surface phenotype (CD45RA$^+$CCR7$^+$CD38$^+$) and included a prominent subset of CD4$^+$ cells. It is noteworthy that these MR1T cells rapidly lost expression of CD45RA, CCR7 and CD38 and acquired a phenotype consistent with those observed in antigen-experienced memory T cells much more rapidly than other types of T cells (Chua et al., 2012; Tsukamoto et al., 2013; Lindestam Arlehamn et al., 2014).

While Koay *et al* showed the functional potential of neonatal MR1T cells that produced TNF following stimulation with PMA/Ionomycin, we show for the first time the presence of functional microbe-reactive MR1T cells in neonates, albeit at low frequency. Virtually all of the mycobacteria-reactive TNF-producing MR1T cells were contained within the TRAV1-2$^+$CD161^{++}CD26^{++} subset of 5-OP-RU tetramer$^+$ cells, which are also concordant with "Stage 3" MR1T cells defined by Koay *et al*. Although the immature CD4$^+$, CD4-CD8- and/or TRAV1-2- MR1T cells were maintained through to adulthood, we observed that CD8$^+$TRAV1-2$^+$ MR1T cells expanded preferentially over TRAV1-2$^-$ MR1T cells. This expansion coincided with the acquisition of high expression of CD26 and CD161 as markers of mature functional MR1 T cells. Of note, studies evaluating the development of CD8$^+$CD161^{++} T cells in humans reported that a lower proportion of this cell population expressed TRAV1-2 in neonates as compared to 2 year-olds (Fergusson et al., 2014) and adults (Walker et al., 2012; Fergusson et al., 2014), and that in adults, CD8$^+$CD161^{++} T cells producing IFN-γ in response to *E. coli* expressed TRAV1-2 (Fergusson et al., 2014). While these studies did not use the MR1 tetramer, these findings are consistent with our results to the extent that the total CD8$^+$ CD161^{++} population reflected MR1T cells. In addition, we show that the frequency of these functional mycobacterial-reactive MR1T cells increases ~10-fold in the first year of life. A surprising finding was that given a comparable stimulus (PMA/Ionomycin and *M. smegmatis*), the infant MR1T cells exhibited a higher functional capacity than the adults. Interestingly, we demonstrated that relative to other T cell subsets, MR1T cells had the highest capacity to secrete the pro-inflammatory cytokine, TNF, in infants. Thus, MR1T cells may represent an important source of pro-inflammatory effectors in infants, who are more vulnerable to serious bacterial infections in the first two years of life, relative to older children and adults.

317 Regarding newborns, it is not known to what degree the naïve phenotype and low
318 functionality of MR1T cells contributes to the very high susceptibility to bacterial infection in the
319 first two months of life (Paul K Sue, 2018). Since MR1T cells recognize important childhood
320 bacterial pathogens, including *S. aureus, S. pneumoniae and enteric pathogens (e.g. E. coli,*
321 *Klebsiella, Salmonella species*, it is plausible that the low frequency of functional MR1T cells
322 during the neonatal period contributes to neonatal susceptibility to infection. At the very least, our
323 findings add to the well-described differences in adaptive and innate immunity between neonates
324 and adults (Paul K Sue, 2018).

325 With regard to *M. tuberculosis*, there is mounting evidence that supports an important host
326 defense role for MR1T cells, especially during early infection. Upon encounter with
327 mycobacterial-infected cells, MR1T cells produce pro-inflammatory cytokines such as IFN-γ and
328 TNF (Gold et al., 2010), known to be essential mediators to host defense against *M. tuberculosis*
329 (Lindestam Arlehamn et al., 2014). MR1-deficient mice control BCG less well than wild type
330 mice (Chua et al., 2012). In humans, MR1 polymorphisms are associated with susceptibility to TB
331 meningitis (Seshadri et al., 2017). It is tempting to speculate, in light of the high susceptibility of
332 infants to TB, and the phenotypic and functional attributes of MR1T cells we observed, that MR1T
333 cells contribute to control of early infection with *M. tuberculosis* through their early and robust
334 anti-mycobacterial response, particularly in the lung.

335 **Methods**

336 **Study participants**

337 **University of Cape Town, Western Cape, South Africa.** All participants were enrolled either at
338 the South African Tuberculosis Vaccine Initiative Field Site, Well-Baby Clinics or Maternity
339 Wards in the Worcester region, near Cape Town, South Africa. Pregnant mothers were enrolled
340 for collection of cord blood immediately after childbirth by Cesarean section. Mothers who may
341 have been exposed to *M. tuberculosis*, HIV infected, had any other acute or chronic disease, and
342 receiving medication other than anesthetic given during delivery were excluded. Infants born to
343 HIV negative mothers, and who had received BCG at birth, had no perinatal complications, or
344 household contact with any person with TB, and did not have any acute or chronic disease were
345 enrolled for collection of blood. Healthy adolescents of 12-18 years of age without evidence of
346 latent Mtb infection as determined by positivity negativity for the Tuberculin Skin Test (<10mm)
347 or QuantiFERON (<0.35IU/mL) were enrolled for blood collection. Heparinized blood was
348 collected for cord blood mononuclear cell (CBMC) and peripheral blood mononuclear cells
349 (PBMC) isolation by means of density gradient centrifugation.

350 **Oregon Health and Science University, Portland, OR, USA.** Umbilical cord blood was obtained
351 from the placenta of uncomplicated term pregnancies after delivery into citrate CPT tubes (BD).
352 Blood was processed per manufacturer's instructions within 24hr of collection, and resulting
353 CBMC cryopreserved. Infants aged 1-24 months undergoing elective surgery at OHSU
354 Doernbecher Children's Hospital were enrolled. Infants had not received BCG vaccination, which
355 is not part of the childhood immunization series in the United States. Blood was drawn into citrate
356 CPT tubes (BD) and processed per manufacturer's instructions to isolate PBMC within 24hr of
357 collection, and PBMC subsequently cryopreserved. Adult PBMC were obtained by leukapheresis
358 from healthy adult donors and cryopreserved. Adult participants lacked any detectable responses
359 to *Mycobacterium tuberculosis* (Mtb) immunodominant antigens CFP-10 and ESAT-6 and
360 therefore were assumed to be Mtb uninfected.

361 **Makerere University, Kampala, Uganda.** Children from age 2-60 months hospitalized with
362 lower respiratory infection (LRTI) from etiologies other than TB were recruited from Mulago
363 Hospital Paediatric Wards. All children were HIV-negative and had no known recent TB contacts.
364 Children were reassessed two months following enrollment to establish vital status and ensure
365 clinical improvement. Following completion of the study, data from all participating children was
366 reviewed by study investigators (DAL, CLL, SK) to confirm diagnosis of non-TB LRTI. Blood
367 was drawn into citrate CPT tubes (BD) and processed per manufacturer's instructions to isolate
368 PBMC within 24hr of collection, and PBMC subsequently cryopreserved. Adult participants were
369 recruited from the National TB Treatment Center at Mulago Hospital, hospital staff, and the
370 community surrounding Kampala, Uganda, between 2001 and 2014. Participants were HIV
371 uninfected and included individuals with (tuberculin skin test, TST ≥ 10) or without (TST < 10
372 mm) evidence of Mtb infection. All had the absence of signs or symptoms of TB (prolonged cough,
373 hemoptysis, fever, weight loss, and night sweats). Heparinized blood was collected for PBMC
374 isolation by means of density gradient centrifugation.

375 **Study approvals**

The studies of all participants were conducted in accordance with the World's Medical Association's Declaration of Helsinki guidelines. The studies from the Western Cape, South Africa were approved by the Human Research Ethics Committee (HREC) of the University of Cape Town. Written informed consent was obtained from parents or legal guardians of adolescents and infants. Adolescents also provided written informed assent. The Institutional Review Board of Oregon Health & Science University (Portland, Oregon) approved this study of participants from Portland, OR. Written, informed consent was obtained from all adult participants and from a parent or legal guardian of infants before enrollment. For participants from Kampala, Uganda, the National Council for Science and Technology, HIV/AIDS Research Committee in Uganda, the Institutional Review Board of Oregon Health & Sciences University (Portland, OR) and the Institutional Review Board of Makerere University (Kampala, Uganda) approved this study. Written, informed consent was obtained from all adult participants and from a parent or legal guardian of infants and children before enrollment.

Infection of antigen presenting cells

A549 cells (ATCC CCL-185) were used as stimulators for direct ex vivo determination of mycobacterial-reactive T cells. *Mycobacterium smegmatis* (strain mc^2155, ATCC) was grown to OD600 of 0.5 and frozen down. This was functionally titered in this assay to find the optimal amount of *M. smegmatis* (4.13µl/ml) that elicited a strong response in an adult control donor but did not reduce the viability of the antigen presenting cells. A549 cells were seeded in T25 flasks at 1.25e6 in 7.5ml of antibiotic free media. After allowing cells to adhere for 3 hours, the flasks were infected with 31µl of *M. smegmatis*. After 18 h, the cells were harvested and washed twice in RPMI/10% human serum containing antibiotic (gentamicin) before being resuspended in RPMI/10% human serum containing antibiotic (gentamicin).

Flow cytometry assays

To perform ICS, cryopreserved PBMC were thawed in the presence of DNAse, resuspended, in 10% heat inactivated human serum with RPMI (Lonza) at a concentration of 2 x 10^7/ml. PBMC (2 x 10^6 cells/well) were stimulated with anti-CD28 (1 µg/ml) and anti-CD49d (1 µg/ml) (FastImmune, BD Biosciences) and 1e5 *M. smegmatis*-infected or uninfected A549 cells in RPMI/10% Human Serum for 18 h at 37°C with 5% $C0_2$. During the last 12 h of this incubation, Brefeldin-A (5 µg/ml) was added. PBMC incubated with uninfected A549 cells were used to assess for background cytokine production. To determine the total functional capacity of T cells, PBMC were incubated with uninfected A549 cells and PMA/Ionomycin (PMA, 20ng/ml, Sigma; Ionomycin, 1µM, Sigma) for 3 hr. PBMC were then harvested and stained with MR1-5-OP-RU or MR1-6FP tetramers (Corbett et al., 2014) (NIH Tetramer Core) at a 1:500 dilution for 45 minutes at room temperature. All tetramers used were conjugated to R-phycoerythrin (PE) or Brilliant Violet (BV) 421. After 45 minutes, an antibody cocktail containing LIVE/DEAD Fixable Dead Cell Stain Kit (Thermo Fisher), and the surface antibodies listed in S1 Table were added for 30 minutes at 4°C. After washing, cells were fixed and permeabilized using Cytofix/Cytoperm (BD Biosciences) per manufacturer's instructions. Cells were then stained for CD3 and TNF, then fixed in 1% PFA. Acquisition was performed using a (Beckman Coulter) Cytoflex flow cytometer with

416 CytExpert software (BC). All flow cytometry data was analyzed using FlowJo software (TreeStar)
417 and Prism (Graphpad).

418 To perform cell surface staining for phenotyping MR1T cells, cryopreserved PBMC were
419 thawed as described above, and 1-2 x 10^6 PBMC were stained with MR1/5-OP-RU or MR1/6FP
420 tetramers at 1:500 for 45 minutes at room temperature. Cells were then subsequently stained with
421 an antibody cocktail containing LIVE/DEAD Fixable Dead Cell Stain Kit (Thermo Fisher), and
422 surface stained with the antibodies listed in S2-S4 Tables for 30 minutes at 4°C. Samples were
423 washed and fixed with 1% PFA. Acquisition of the US samples was performed using a Cytoflex
424 flow cytometer (Beckman) with CytExpert software (BC). For experiments with the Ugandan
425 samples, acquisition was performed on a BD LSRFortessa. For experiments performed at SATVI,
426 samples were acquired on a BD LSR-II flow cytometer configured with 4 lasers: solid state blue
427 (488nm; 100mW; 3 detectors), solid state violet (405nm; 25mW; 8 detectors), HeNe gas red
428 (635nm; 70mW; 3 detectors), and diode-pumped Coherent Compass yellow-green (532nm;
429 150mW; 8 detectors). Flow cytometric analysis was performed using FlowJo version 10.5.3
430 (Treestar, Ashland, OR, USA).

431 **Data analysis and Statistics**

432 Adjusted frequency (raw frequency of cytokine production following stimulation minus
433 the frequency of cytokine production in resting/unstimulated condition), was used to account for
434 the potential presence of background, or non-specific, responses. A positive cytokine response was
435 defined as the detection of at least 0.05% cytokine-positive T cells (following background
436 subtraction). Prism version 7 (GraphPad, La Jolla, CA, USA) was used for data analysis. A p-value
437 < 0.05 was considered as statistically significant.

438 To characterize phenotypic diversity within MR1T cell populations at the different ages
439 we performed t-Stochastic Neighbor Embedding (tSNE) on MR1-5-OP-RU tetramer$^+$ defined
440 CD3$^+$ T cells. Data from MR1-5-OP-RU tetramer$^+$ cells from all individuals across the age groups
441 were concatenated into a single FCS file to perform tSNE analysis in FlowJo. Equal event sampling
442 was not performed due to low events per individual in the cord blood and infant samples.
443 Clustering analysis was performed based on the expression of five surface markers (CD4, CD8,
444 TRAV1-2, CD26, and CD161). Parameter settings were fixed at 2000 iterations with a learning
445 rate (Eta) of 10 and perplexity 30, respectively (van der Maaten and Hinton, 2008).

446 **Conflict of Interest statement**

447 The authors declare that the research was conducted in the absence of any commercial or financial
448 relationships that could be construed as a potential conflict of interest.

Author Contributions

GMS, AG, DML, TJS and DAL contributed to the conception and/or design of the work. GMS and AG are joint first authors. TJS and DAL jointly supervised the work. MN, HMK, SK, JK, CL, EN, MS, WAH, MH and TJS contributed to clinical activities. EN, WAH, MH, DML, DAL and TJS raised grants to fund the research. GMS, AG, MEC, MDN, RBD, DML, TJS and DAL substantially contributed to the acquisition, analysis or interpretation of data and drafting of the manuscript. All authors substantially contributed to revising and critically reviewing the manuscript for important intellectual content. All authors approved the final version of this manuscript to be published and agree to be accountable for all aspects of the work.

Funding

This project has been funded in whole or in part with Federal funds from the National Institutes of Allergy and Infectious Diseases, National Institutes of Health, Department of Health and Human Services, under grant no R01 AI04229 and contract HHSN272200900053C.

Work at SATVI was supported by Aeras, the National Institutes of Health Grant R01-AI087915 and R01-AI065653 and the European and Developing Countries Clinical Trial Partnership. Anele Gela was supported by a Postdoctoral Fellowship from the Claude Leon Foundation.

The funders had no role in study design, data collection and analysis, decision to publish, or preparation of the manuscript.

468 **Acknowledgments**

469 We would like to thank the participants who gave time and dedication to this health
470 research; W. Henry Boom, LaShaunda Malone and Keith Chervenak, Case Western Reserve
471 University; and Erin Merrifield, Department of Pediatrics, OHSU, for their contributions to this
472 study.

473 The MR1 tetramer technology was developed jointly by Dr. James McCluskey, Dr. Jamie
474 Rossjohn, and Dr. David Fairlie, and the material was produced by the NIH Tetramer Core Facility
475 as permitted to be distributed by the University of Melbourne.

476 This manuscript has been released as a pre-print at bioRxiv, (Swarbrick et al., 2019).

477 **References**

478 Ben Youssef, G., Tourret, M., Salou, M., Ghazarian, L., Houdouin, V., Mondot, S., et al. (2018).
479 Ontogeny of human mucosal-associated invariant T cells and related T cell subsets. *Journal*
480 *of Experimental Medicine* 215(2)**,** 459-479. doi: 10.1084/jem.20171739.
481 Chua, W.J., Truscott, S.M., Eickhoff, C.S., Blazevic, A., Hoft, D.F., and Hansen, T.H. (2012).
482 Polyclonal Mucosa-Associated Invariant T Cells Have Unique Innate Functions in
483 Bacterial Infection. *Infection and Immunity* 80(9)**,** 3256-3267. doi: 10.1128/Iai.00279-12.
484 Constantinides, M.G., Link, V.M., Tamoutounour, S., Wong, A.C., Perez-Chaparro, P.J., Han,
485 S.J., et al. (2019). MAIT cells are imprinted by the microbiota in early life and promote
486 tissue repair. *Science* 366(6464). doi: 10.1126/science.aax6624.
487 Corbett, A.J., Eckle, S.B.G., Birkinshaw, R.W., Liu, L.G., Patel, O., Mahony, J., et al. (2014).
488 T-cell activation by transitory neo-antigens derived from distinct microbial pathways.
489 *Nature* 509(7500)**,** 361-+. doi: 10.1038/nature13160.
490 Dusseaux, M., Martin, E., Serriari, N., Peguillet, I., Premel, V., Louis, D., et al. (2011). Human
491 MAIT cells are xenobiotic-resistant, tissue-targeted, CD161hi IL-17-secreting T cells.
492 *Blood* 117(4)**,** 1250-1259. doi: 10.1182/blood-2010-08-303339.
493 Eckle, S.B., Birkinshaw, R.W., Kostenko, L., Corbett, A.J., McWilliam, H.E., Reantragoon, R.,
494 et al. (2014). A molecular basis underpinning the T cell receptor heterogeneity of mucosal-
495 associated invariant T cells. *J Exp Med* 211(8)**,** 1585-1600. doi: 10.1084/jem.20140484.
496 Fergusson, J.R., Smith, K.E., Fleming, V.M., Rajoriya, N., Newell, E.W., Simmons, R., et al.
497 (2014). CD161 Defines a Transcriptional and Functional Phenotype across Distinct Human
498 T Cell Lineages. *Cell Reports* 9(3)**,** 1075-1088. doi: 10.1016/j.celrep.2014.09.045.
499 Georgel, P., Radosavljevic, M., Macquin, C., and Bahram, S. (2011). The non-conventional
500 MHC class I MR1 molecule controls infection by Klebsiella pneumoniae in mice. *Mol*
501 *Immunol* 48(5)**,** 769-775. doi: 10.1016/j.molimm.2010.12.002.
502 Gherardin, N.A., Keller, A.N., Woolley, R.E., Le Nours, J., Ritchie, D.S., Neeson, P.J., et al.
503 (2016). Diversity of T Cells Restricted by the MHC Class I-Related Molecule MR1
504 Facilitates Differential Antigen Recognition. *Immunity* 44(1)**,** 32-45. doi:
505 10.1016/j.immuni.2015.12.005.
506 Gherardin, N.A., Souter, M.N.T., Koay, H.F., Mangas, K.M., Seemann, T., Stinear, T.P., et al.
507 (2018). Human blood MAIT cell subsets defined using MR1 tetramers. *Immunology and*
508 *Cell Biology* 96(5)**,** 507-525. doi: 10.1111/imcb.12021.
509 Godfrey, D.I., Koay, H.F., McCluskey, J., and Gherardin, N.A. (2019). The biology and
510 functional importance of MAIT cells. *Nat Immunol* 20(9)**,** 1110-1128. doi:
511 10.1038/s41590-019-0444-8.
512 Gold, M.C., Cerri, S., Smyk-Pearson, S., Cansler, M.E., Vogt, T.M., Delepine, J., et al. (2010).
513 Human mucosal associated invariant T cells detect bacterially infected cells. *PLoS Biol*
514 8(6)**,** e1000407. doi: 10.1371/journal.pbio.1000407.
515 Gold, M.C., Eid, T., Smyk-Pearson, S., Eberling, Y., Swarbrick, G.M., Langley, S.M., et al.
516 (2013). Human thymic MR1-restricted MAIT cells are innate pathogen-reactive effectors
517 that adapt following thymic egress. *Mucosal Immunology* 6(1)**,** 35-44. doi:
518 10.1038/mi.2012.45.

Harriff, M.J., McMurtrey, C., Froyd, C.A., Jin, H.H., Cansler, M., Null, M., et al. (2018). MR1 displays the microbial metabolome driving selective MR1-restricted T cell receptor usage. *Science Immunology* 3(25). doi: UNSP eaao2556 10.1126/sciimmunol.aao2556.

Hartmann, N., Harriff, M.J., McMurtrey, C.P., Hildebrand, W.H., Lewinsohn, D.M., and Kronenberg, M. (2018). Role of MAIT cells in pulmonary bacterial infection. *Mol Immunol* 101**,** 155-159. doi: 10.1016/j.molimm.2018.06.270.

Kjer-Nielsen, L., Patel, O., Corbett, A.J., Le Nours, J., Meehan, B., Liu, L., et al. (2012). MR1 presents microbial vitamin B metabolites to MAIT cells. *Nature* 491(7426)**,** 717-723. doi: 10.1038/nature11605.

Koay, H.F., Gherardin, N.A., Enders, A., Loh, L., Mackay, L.K., Almeida, C.F., et al. (2016). A three-stage intrathymic development pathway for the mucosal-associated invariant T cell lineage. *Nature Immunology* 17(11)**,** 1300-1311. doi: 10.1038/ni.3565.

Koay, H.F., Godfrey, D.I., and Pellicci, D.G. (2018). Development of mucosal-associated invariant T cells. *Immunology and Cell Biology* 96(6)**,** 598-606. doi: 10.1111/imcb.12039.

Kurioka, A., Ussher, J.E., Cosgrove, C., Clough, C., Fergusson, J.R., Smith, K., et al. (2015). MAIT cells are licensed through granzyme exchange to kill bacterially sensitized targets. *Mucosal Immunology* 8(2)**,** 429-440. doi: 10.1038/mi.2014.81.

Le Bourhis, L., Dusseaux, M., Bohineust, A., Bessoles, S., Martin, E., Premel, V., et al. (2013). MAIT Cells Detect and Efficiently Lyse Bacterially-Infected Epithelial Cells. *Plos Pathogens* 9(10). doi: ARTN e1003681 10.1371/journal.ppat.1003681.

Legoux, F., Bellet, D., Daviaud, C., El Morr, Y., Darbois, A., Niort, K., et al. (2019). Microbial metabolites control the thymic development of mucosal-associated invariant T cells. *Science* 366(6464)**,** 494-499. doi: 10.1126/science.aaw2719.

Lepore, M., Kalinicenko, A., Colone, A., Paleja, B., Singhal, A., Tschumi, A., et al. (2014). Parallel T-cell cloning and deep sequencing of human MAIT cells reveal stable oligoclonal TCR beta repertoire. *Nature Communications* 5. doi: ARTN 3866 10.1038/ncomms4866.

Lindestam Arlehamn, C.S., Lewinsohn, D., Sette, A., and Lewinsohn, D. (2014). Antigens for CD4 and CD8 T cells in tuberculosis. *Cold Spring Harb Perspect Med* 4(7)**,** a018465. doi: 10.1101/cshperspect.a018465.

Marais, B.J., Gie, R.P., Schaaf, H.S., Hesseling, A.C., Enarson, D.A., and Beyers, N. (2006). The spectrum of disease in children treated for tuberculosis in a highly endemic area. *International Journal of Tuberculosis and Lung Disease* 10(7)**,** 732-738.

Marais, B.J., Gie, R.P., Schaaf, H.S., Hesseling, A.C., Obihara, C.C., Nelson, L.J., et al. (2004a). The clinical epidemiology of childhood pulmonary tuberculosis: a critical review of literature from the pre-chemotherapy era. *International Journal of Tuberculosis and Lung Disease* 8(3)**,** 278-285.

Marais, B.J., Gie, R.R., Schaaf, H.S., Hesseling, A.C., Obihara, C.C., Starke, J.J., et al. (2004b). The natural history of childhood intra-thoracic tuberculosis: a critical review of literature from the pre-chemotherapy era. *International Journal of Tuberculosis and Lung Disease* 8(4)**,** 392-402.

562 Martin, E., Treiner, E., Duban, L., Guerri, L., Laude, H., Toly, C., et al. (2009). Stepwise
563 Development of MAIT Cells in Mouse and Human. *Plos Biology* 7(3)**,** 525-536. doi:
564 ARTN e1000054
565 10.1371/journal.pbio.1000054.
566 Meermeier, E.W., Laugel, B.F., Sewell, A.K., Corbett, A.J., Rossjohn, J., McCluskey, J., et al.
567 (2016). Human TRAV1-2-negative MR1-restricted T cells detect S-pyogenes and
568 alternatives to MAIT riboflavin-based antigens. *Nature Communications* 7. doi: ARTN
569 12506
570 10.1038/ncomms12506.
571 Meierovics, A., Yankelevich, W.J.C., and Cowley, S.C. (2013). MAIT cells are critical for
572 optimal mucosal immune responses during in vivo pulmonary bacterial infection.
573 *Proceedings of the National Academy of Sciences of the United States of America* 110(33)**,**
574 E3119-E3128. doi: 10.1073/pnas.1302799110.
575 Meierovics, A.I., and Cowley, S.C. (2016). MAIT cells promote inflammatory monocyte
576 differentiation into dendritic cells during pulmonary intracellular infection. *Journal of*
577 *Experimental Medicine* 213(12)**,** 2793-2809. doi: 10.1084/jem.20160637.
578 Paul K Sue, M.M., and Maite de la Morena (2018). "Immunologic Development and
579 Susceptibility to Infection.," in *Principles and Practice of Pediatric Infectious Diseases.*
580 *5th ed.,* ed. G.C.P. S. Sarah Long, M. Fischer.: Elsevier), p85-92.
581 Reantragoon, R., Corbett, A.J., Sakala, I.G., Gherardin, N.A., Furness, J.B., Chen, Z.J., et al.
582 (2013). Antigen-loaded MR1 tetramers define T cell receptor heterogeneity in mucosal-
583 associated invariant T cells. *Journal of Experimental Medicine* 210(11)**,** 2305-2320. doi:
584 10.1084/jem.20130958.
585 Sakala, I.G., Kjer-Nielsen, L., Eickhoff, C.S., Wang, X., Blazevic, A., Liu, L., et al. (2015).
586 Functional Heterogeneity and Antimycobacterial Effects of Mouse Mucosal-Associated
587 Invariant T Cells Specific for Riboflavin Metabolites. *J Immunol* 195(2)**,** 587-601. doi:
588 10.4049/jimmunol.1402545.
589 Sattler, A., Dang-Heine, C., Reinke, P., and Babel, N. (2015). IL-15 dependent induction of IL-
590 18 secretion as a feedback mechanism controlling human MAIT-cell effector functions.
591 *Eur J Immunol* 45(8)**,** 2286-2298. doi: 10.1002/eji.201445313.
592 Seshadri, C., Thuong, N.T.T., Mai, N.T.H., Bang, N.D., Chau, T.T.H., Lewinsohn, D.M., et al.
593 (2017). A polymorphism in human MR1 is associated with mRNA expression and
594 susceptibility to tuberculosis. *Genes and Immunity* 18(1)**,** 8-14. doi: 10.1038/gene.2016.41.
595 Sharma, P.K., Wong, E.B., Napier, R.J., Bishai, W.R., Ndung'u, T., Kasprowicz, V.O., et al.
596 (2015). High expression of CD26 accurately identifies human bacteria-reactive MR1-
597 restricted MAIT cells. *Immunology* 145(3)**,** 443-453. doi: 10.1111/imm.12461.
598 Slichter, C.K., McDavid, A., Miller, H.W., Finak, G., Seymour, B.J., McNevin, J.P., et al. (2016).
599 Distinct activation thresholds of human conventional and innate-like memory T cells. *JCI*
600 *Insight* 1(8). doi: 10.1172/jci.insight.86292.
601 Suliman, S., Gela, A., Mendelsohn, S.C., Iwany, S.K., Tamara, K.L., Mabwe, S., et al. (2020).
602 Peripheral blood mucosal-associated invariant T (MAIT) cells in tuberculosis patients and
603 healthy Mycobacterium tuberculosis-exposed controls. *J Infect Dis*. doi:
604 10.1093/infdis/jiaa173.

605 Swarbrick, G.M., Gela, A., Cansler, M.E., Null, M.D., Duncan, R.B., Nemes, E., et al. (2019).
606 Postnatal expansion, maturation and functionality of MR1 T cells in humans. *bioRxiv*,
607 2019.2012.2020.882746. doi: 10.1101/2019.12.20.882746.
608 Treiner, E., Duban, L., Bahram, S., Radosavljevic, M., Wanner, V., Tilloy, F., et al. (2003).
609 Selection of evolutionarily conserved mucosal-associated invariant T cells by MR1 (vol
610 422, pg 164, 2003). *Nature* 423(6943), 1018-1018. doi: 10.1038/nature01700.
611 Tsukamoto, K., Deakin, J.E., Graves, J.A.M., and Hashimoto, K. (2013). Exceptionally high
612 conservation of the MHC class I-related gene, MR1, among mammals. *Immunogenetics*
613 65(2), 115-124. doi: 10.1007/s00251-012-0666-5.
614 Ussher, J.E., Bilton, M., Attwod, E., Shadwell, J., Richardson, R., de Lara, C., et al. (2014).
615 CD161++ CD8+ T cells, including the MAIT cell subset, are specifically activated by IL-
616 12+IL-18 in a TCR-independent manner. *Eur J Immunol* 44(1), 195-203. doi:
617 10.1002/eji.201343509.
618 van der Maaten, L., and Hinton, G. (2008). Visualizing Data using t-SNE. *Journal of Machine*
619 *Learning Research* 9, 2579-2605.
620 van Wilgenburg, B., Scherwitzl, I., Hutchinson, E.C., Leng, T., Kurioka, A., Kulicke, C., et al.
621 (2016). MAIT cells are activated during human viral infections. *Nat Commun* 7, 11653.
622 doi: 10.1038/ncomms11653.
623 Walker, L.J., Kang, Y.H., Smith, M.O., Tharmalingham, H., Ramamurthy, N., Fleming, V.M.,
624 et al. (2012). Human MAIT and CD8alphaalpha cells develop from a pool of type-17
625 precommitted CD8+ T cells. *Blood* 119(2), 422-433. doi: 10.1182/blood-2011-05-353789.
626 Walker, L.J., Tharmalingam, H., and Klenerman, P. (2014). The Rise and Fall of MAIT Cells
627 with Age. *Scandinavian Journal of Immunology* 80(6), 462-463. doi: 10.1111/sji.12237.
628 Wang, H.M., D'Souza, C., Lim, X.Y., Kostenko, L., Pediongco, T.J., Eckle, S.B.G., et al. (2018).
629 MAIT cells protect against pulmonary Legionella longbeachae infection. *Nature*
630 *Communications* 9. doi: ARTN 3350
631 10.1038/s41467-018-05202-8.
632 Zar, H.J., and Ferkol, T.W. (2014). The global burden of respiratory disease-impact on child
633 health. *Pediatr Pulmonol* 49(5), 430-434. doi: 10.1002/ppul.23030.
634

635 **Figure Legends**

636 **Figure 1. Frequencies of tetramer-defined MR1T cell and phenotypically defined MAIT cell**
637 **populations in peripheral blood from individuals of different ages.** PBMC or CBMC were
638 stained with a live/dead discriminator, antibodies to CD3, CD4, CD8, TRAV1-2, CD26, CD161,
639 and either the MR1-5-OP-RU or MR1-6FP tetramers. Live, $CD3^+$ lymphocytes were gated and the
640 frequencies of MR1-5-OP-RU^+ or TRAV1-$2^+CD161^{++}CD26^{++}$ cells as a percentage of $CD3^+$
641 lymphocytes were determined (gating strategy in Figure S2). **A**. Flow cytometry plots showing
642 $CD3^+$ T cell staining with MR1-5-OP-RU tetramer, MR1-6FP tetramer, TRAV1-2 or
643 CD26/CD161 of samples from a representative US adult, infant and neonate. **B.** Frequencies of
644 tetramer-defined ($CD3^+$MR1-5-OP-RU^+) and phenotypically-defined ($CD3^+$TRAV1-2^+
645 $CD161^{++}CD26^{++}$) MAIT cells in neonates, 10 week-old infants and adolescents from South Africa,
646 neonates, 12 month-old infants and adults from the United States and infants (0-2 years old),
647 children (2-5 years old) and adults from Uganda (all cohorts, *n*=10). Mann-Whitney u-tests were
648 used to test differences between groups. Horizontal lines depict the median and the error bars the
649 95% confidence interval. **C.** Relative proportions of median phenotypically-defined
650 ($CD3^+$TRAV1-$2^+CD161^{++}CD26^{++}$) MAIT cells that are MR1-5-OP-RU^+ (Blue) and MR1-5-OP-
651 RU^- (Red) for each age group at each site.

652 **Figure 2. Functional analysis of MAIT cells in individuals of different ages.** PBMC or CBMC
653 from the US cohort were incubated overnight with *M. smegmatis*-infected A549 cells or uninfected
654 A549 cells and then stained with the MR1-5-OP-RU or MR1-6FP tetramers, followed by staining
655 with a live/dead discriminator and antibodies to TCRγδ, CD3, CD4, CD8, TRAV1-2, CD26 and
656 CD161. ICS was then performed and the cells stained for TNF. **A.** Dot plots showing representative
657 co-staining of live, $TCR\gamma\delta^-CD3^+$TRAV1-$2^+CD161^{++}CD26^{++}$ cells with MR1-5-OP-RU and TNF
658 in *M. smegmatis* stimulated or unstimulated samples. The gating strategy is in Figure S5. Examples
659 of the TNF response in a neonate, infant and adult are shown. **B.** Frequencies of phenotypically-
660 defined ($CD3^+$TRAV1-$2^+CD161^{++}CD26^{++}$) MAIT cells that are TNF^+MR1-5-OP-RU^+ or
661 TNF^+MR1-5-OP-RU^- are shown. Horizontal lines depict the median and the error bars the 95%
662 confidence interval. Wilcoxon-rank sum was used to test differences within the same cohort.

663 **Figure 3. Phenotypic diversity of MR1T cells in individuals of different ages.** t-Distributed
664 stochastic neighbor embedding (tSNE) plots showing MR1-5-OP-RU $tetramer^+CD3^+$ T cells
665 (gating strategy in Figure S2) from the South African (SA) or United States (US) cohorts (Table1).
666 Plots represent cells from 10 samples from each age group. **A.** and **C.** The five clusters identified
667 in both sites are shown in **A** (SA) and **C** (US). **B.** and **D.** Dot plots colored by the relative
668 expression level of each marker (CD4, CD8, TRAV1-2, CD161 or CD26) in tetramer-defined
669 MR1T cells for each age group in **B** (SA) and **D** (US). Red = highest expression, blue = lowest
670 expression. **E.** and **F.** The proportion of each cluster of tetramer-defined MR1T cells by age group
671 is shown in **E** (SA) and **F** (US). Horizontal lines depict the median and the error bars the 95%
672 confidence interval. Mann-Whitney u tests were used to test differences between groups.

673 **Figure 4. Phenotypic analysis of functional MR1T cells at different ages.** PBMC or CBMC
674 from the US cohort were incubated overnight with *M. smegmatis*-infected A549 cells, uninfected
675 A549 cells, or uninfected A549 cells and PMA/ionomycin. All cells were then stained with the

676 MR1-5-OP-RU or MR1-6FP tetramers, followed by a live/dead discriminator and antibodies to
677 TCRγδ, CD3, CD4, CD8, TRAV1-2, CD26 and CD161. ICS was then performed and the cells
678 stained for TNF. Live, TCRγδ$^-$CD3$^+$MR1-5-OP-RU$^+$ cells were gated and the TNF$^+$ percentage
679 determined in both the *M. smegmatis* stimulated and unstimulated conditions. The gating strategy
680 is shown in Figure S5. **A.** Dot plots showing TNF expression by live, TCRγδ$^-$MR1-5-OP-RU$^+$
681 CD3$^+$ cells in the same representative neonate, infant and adult as Figure 2A. **B.** Background
682 subtracted frequencies of TNF$^+$ MR1-5-OP-RU$^+$ CD3$^+$ cells in response to *M. smegmatis*-infected
683 A549 cells as a percentage of total MR1-5-OP-RU$^+$ CD3$^+$ cells are shown. Mann-Whitney u-tests
684 were used to test differences between groups. **C.** Background subtracted frequencies of TNF$^+$
685 cells to PMA/ionomycin among different T cell subpopulations, 1) MR1T cells (CD3$^+$TCRγδ$^-$
686 MR1-5-OP-RU$^+$ cells); 2) γδ T cells (CD3$^+$TCRγδ$^+$MR1-5-OP-RU$^-$ cells); 3) CD8$^+$ T cells
687 (CD3$^+$TCRγδ$^-$MR1-5-OP-RU$^-$CD8$^+$ cells); and 4) CD4$^+$ T cells (CD3$^+$TCRγδ$^-$MR1-5-OP-RU$^-$
688 CD4$^+$ cells). Wilcoxon-rank sum was used to test differences within the same cohort. **D.** and **E.**
689 Frequencies of TNF$^+$TRAV1-2$^+$ MR1-5-OP-RU$^+$ CD3$^+$ and TNF$^+$TRAV1-2$^-$ MR1-5-OP-RU$^+$
690 CD3$^+$ cells in response to *M. smegmatis* infected A549 cells (**D**) or PMA/ionomycin stimulation
691 (**E**) minus the background frequencies of TNF$^+$TRAV1-2$^+$/- MR1-5-OP-RU$^+$ CD3$^+$ cells.
692 Wilcoxon-rank sum was used to test differences within the same cohort. **F.** and **G.** Frequencies of
693 CD161^{++}CD26^{++} cells of the TNF$^+$TRAV1-2$^+$MR1-5-OP-RU$^+$CD3$^+$ cells in response to *M.*
694 *smegmatis* infected A549 cells (**F**) or PMA/ionomycin stimulation (**G**) are shown. The median and
695 95% confidence intervals are shown in each graph. When the 95% confidence intervals do not
696 overlap between conditions, those conditions are considered statistically significant.

697 **Figure 5. Analysis of MR1T cell development by measuring maturation markers.** PBMC or
698 CBMC from the US were stained as in Figure 1 with the addition of an antibody to CD27. Live,
699 CD3$^+$MR1-5-OP-RU$^+$ cells (gating strategy in Figure S2) were gated for the maturation pattern of
700 S1, S2 and S3 described in (Koay et al., 2016). S1 = CD161$^-$CD27$^-$, S2=CD161$^-$CD27$^+$,
701 S3=CD161$^+$CD27$^{+/-}$. **A.** Gating of MR1T cells for S1, S2 and S3 in a representative neonate, infant
702 and adult. **B.** Frequencies of S1, S2, and S3 MR1T cells as a percentage of CD3$^+$ MR1-5-OP-RU$^+$
703 cells are shown for U.S. neonates, infants and adults. Bars represent the median and the error bars
704 the 95% confidence interval.

705 **Figure 6. Comparative phenotypic analysis of MR1T and non-MR1T cells or TRAV1-2$^+$ and**
706 **TRAV1-2$^-$ MR1T cells at different ages.** PBMC or CBMC from the US were stained as in Figure
707 1 with the addition of antibodies to either CD45RA (**A, B**), CCR7 (**C, D**), CD38 (**E, F**) or CD56
708 (**G, H**). The gating strategy is shown in Figure S2 and examples of the staining of each marker is
709 shown in Figure S6. Frequencies of cells expressing each marker in non-MR1T cells (CD3$^+$MR1-
710 5-OP-RU$^-$) or MR1T cells (CD3$^+$MR1-5-OP-RU$^+$) in each age group (**A, C, E, G**). The frequency
711 of each marker expressed in TRAV1-2$^+$ or TRAV1-2$^-$ MR1T cells is shown in each age group (**B,**
712 **D, F, H**). The median and 95% confidence intervals are shown in each graph. When the 95%
713 confidence intervals do not overlap between conditions, those conditions are considered
714 statistically significant.

715 Tables

716 **Table 1. Study Participants**

Country	*Cohort*	*number*	*Age*	*BCG vaccinated?*	*QFT results*	*TST results*
South Africa	Neonates	10	0 (cord blood)	-	ND	ND
	Infants	10	10 weeks	+	ND	ND
	Adolescents	10	14-18 years	+	-	ND
USA	Neonates	10	0 (cord blood)	-	ND	ND
	Infants	10	9-15 months	-	ND	ND
	Adults	10	29-60 years	-	ND*	ND*
Uganda	Infants	36	2-24 months	+/-	ND	+/-
	Children	23	24-60 months	+/-	ND	+/-
	Adults	91	18-60 years	+/-	ND	+/-

717 ND = Not Done. *While QFT and TST were not performed, the infection status in Oregon is
718 likely to be negative based on epidemiology and results of an in-house ESAT-6/CFP-10 IFN-γ
719 ELISPOT assay.

720

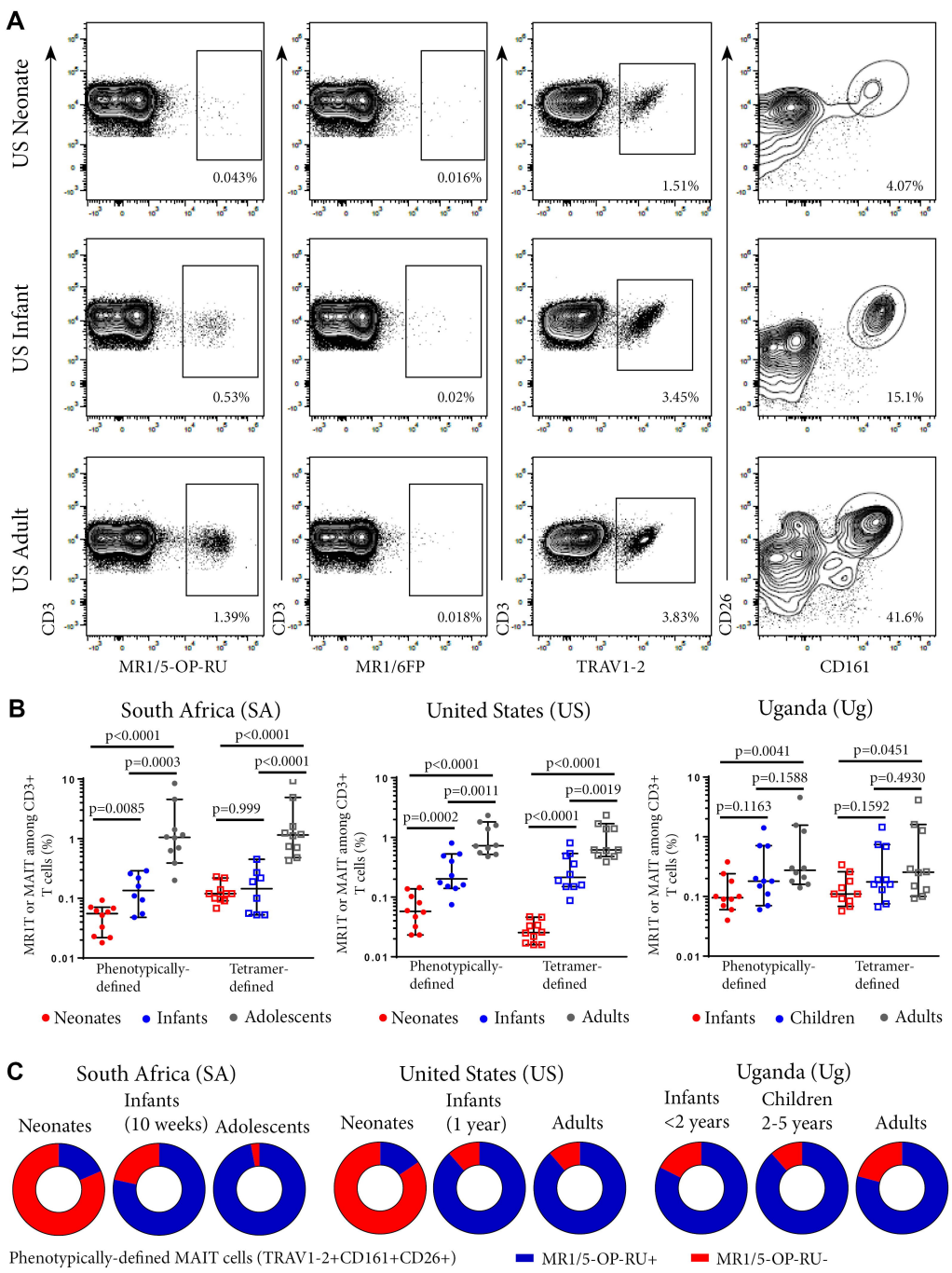
A
US Neonate
US Infant
US Adult
0.043%
0.016%
1.51%
4.07%
0.53%
0.02%
3.45%
15.1%
1.39%
0.018%
3.83%
41.6%
CD3
MR1/5-OP-RU
MR1/6FP
TRAV1-2
CD26
CD161
B
South Africa (SA)
United States (US)
Uganda (Ug)
MR1T or MAIT among CD3+ T cells (%)
p<0.0001
p=0.0003
p=0.0085
p<0.0001
p<0.0001
p=0.999
p<0.0001
p<0.0001
p=0.0011
p=0.0002
p<0.0001
p<0.0001
p=0.0019
p=0.0041
p=0.1588
p=0.1163
p=0.0451
p=0.4930
p=0.1592
Phenotypically-defined
Tetramer-defined
Neonates
Infants
Adolescents
Adults
Children
C
South Africa (SA)
Neonates
Infants (10 weeks)
Adolescents
United States (US)
Neonates
Infants (1 year)
Adults
Uganda (Ug)
Infants <2 years
Children 2-5 years
Adults
Phenotypically-defined MAIT cells (TRAV1-2+CD161+CD26+)
MR1/5-OP-RU+
MR1/5-OP-RU-

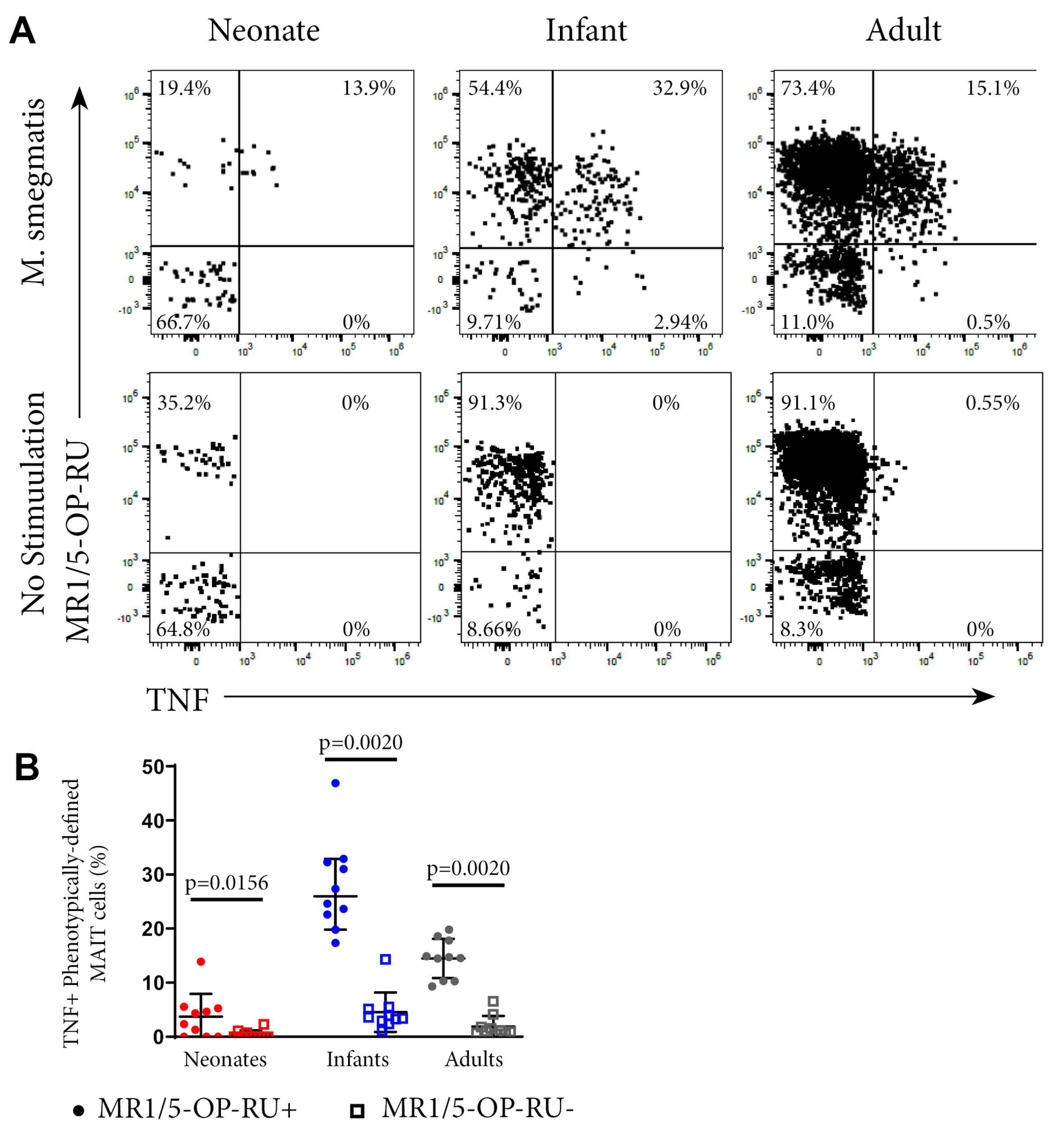
A
Neonate
Infant
Adult
M. smegmatis
No Stimulation
MR1/5-OP-RU
19.4%
13.9%
66.7%
0%
54.4%
32.9%
9.71%
2.94%
73.4%
15.1%
11.0%
0.5%
35.2%
0%
64.8%
0%
91.3%
0%
8.66%
0%
91.1%
0.55%
8.3%
0%
TNF
B
TNF+ Phenotypically-defined MAIT cells (%)
p=0.0156
p=0.0020
p=0.0020
Neonates
Infants
Adults
MR1/5-OP-RU+
MR1/5-OP-RU-

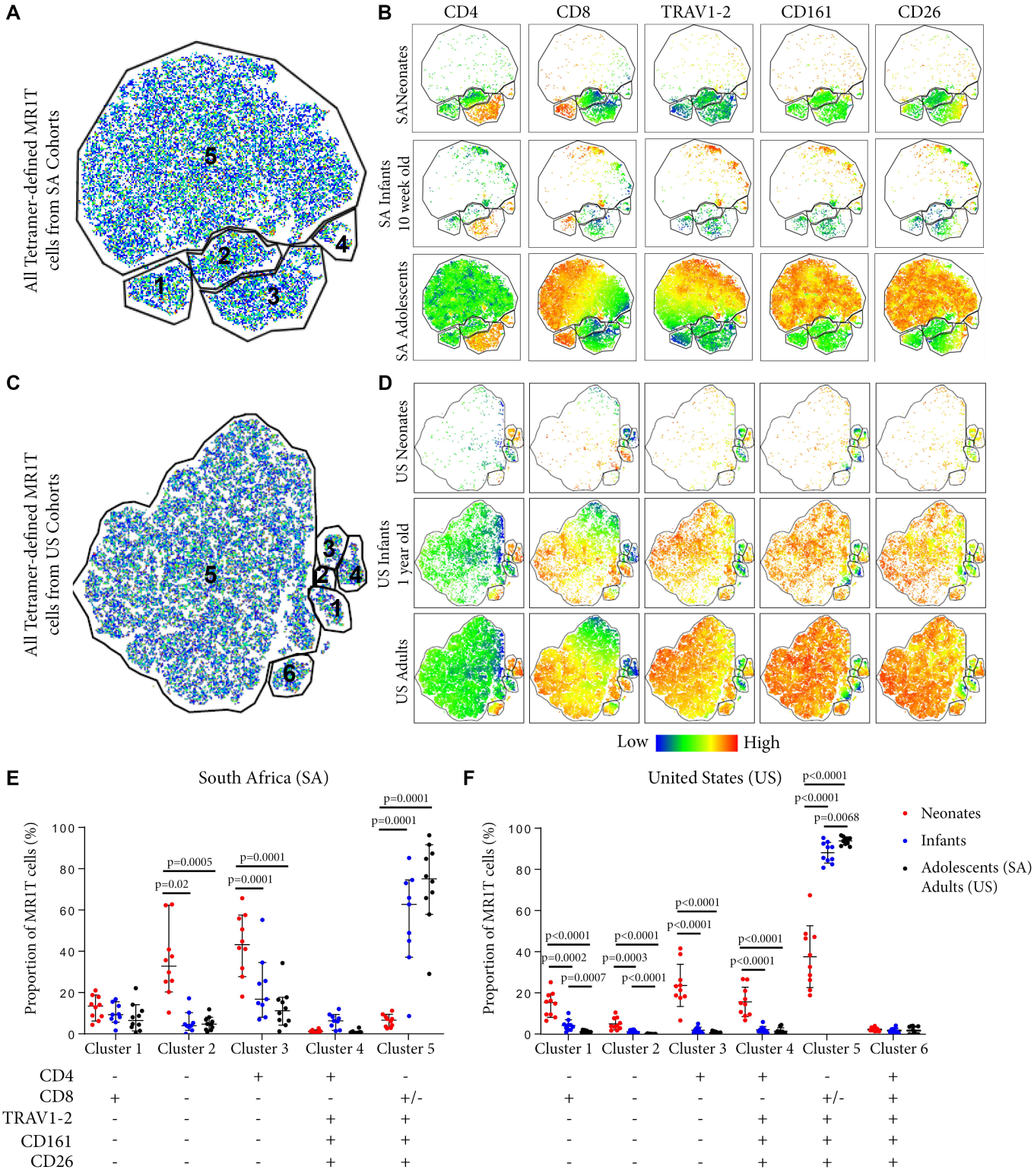
A
All Tetramer-defined MR1T cells from SA Cohorts
1
2
3
4
5
B
CD4
CD8
TRAV1-2
CD161
CD26
SANeonates
SA Infants 10 week old
SA Adolescents
C
All Tetramer-defined MR1T cells from US Cohorts
1
2
3
4
5
6
D
US Neonates
US Infants 1 year old
US Adults
Low
High
E
South Africa (SA)
Proportion of MR1T cells (%)
Cluster 1
Cluster 2
Cluster 3
Cluster 4
Cluster 5
p=0.02
p=0.0005
p=0.0001
p=0.0001
p=0.0001
p=0.0001
p=0.0001
F
United States (US)
Proportion of MR1T cells (%)
Cluster 1
Cluster 2
Cluster 3
Cluster 4
Cluster 5
Cluster 6
p<0.0001
p=0.0002
p=0.0007
p<0.0001
p=0.0003
p<0.0001
p<0.0001
p<0.0001
p<0.0001
p<0.0001
p<0.0001
p<0.0001
p=0.0068
Neonates
Infants
Adolescents (SA)
Adults (US)
CD4 - - + + - - - + + - +
CD8 + - - - +/- + - - - +/- +
TRAV1-2 - - - + + - - - + + +
CD161 - - - + + - - - + + +
CD26 - - - + + - - - + + +

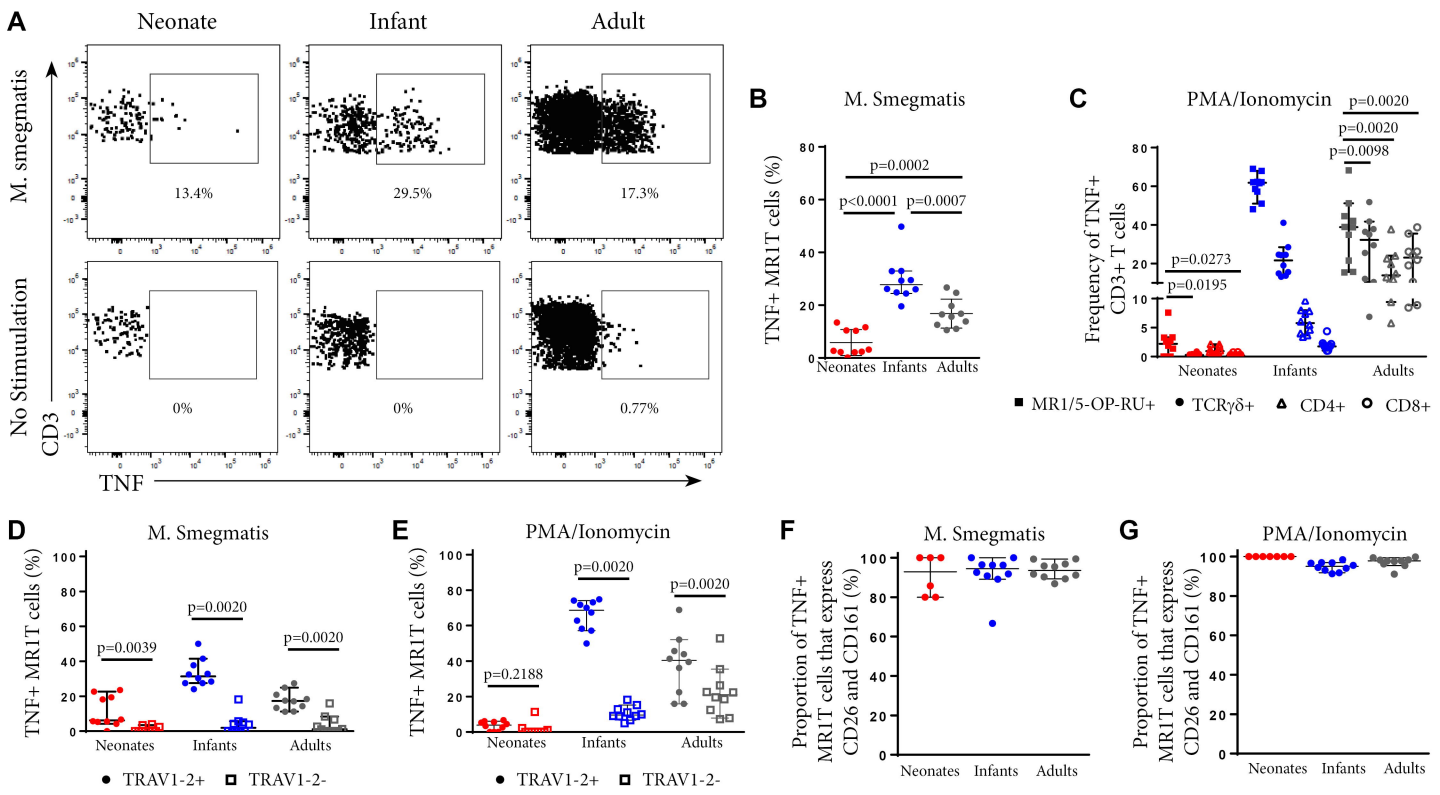
A
Neonate
Infant
Adult
M. smegmatis
No Stimulation
CD3
TNF
13.4%
29.5%
17.3%
0%
0%
0.77%
B
M. Smegmatis
TNF+ MR1T cells (%)
p=0.0002
p<0.0001
p=0.0007
Neonates
Infants
Adults
C
PMA/Ionomycin
Frequency of TNF+ CD3+ T cells
p=0.0020
p=0.0020
p=0.0098
p=0.0273
p=0.0195
Neonates
Infants
Adults
MR1/5-OP-RU+
TCRγδ+
CD4+
CD8+
D
M. Smegmatis
TNF+ MR1T cells (%)
p=0.0039
p=0.0020
p=0.0020
Neonates
Infants
Adults
TRAV1-2+
TRAV1-2-
E
PMA/Ionomycin
TNF+ MR1T cells (%)
p=0.2188
p=0.0020
p=0.0020
Neonates
Infants
Adults
TRAV1-2+
TRAV1-2-
F
M. Smegmatis
Proportion of TNF+ MR1T cells that express CD26 and CD161 (%)
Neonates
Infants
Adults
G
PMA/Ionomycin
Proportion of TNF+ MR1T cells that express CD26 and CD161 (%)
Neonates
Infants
Adults

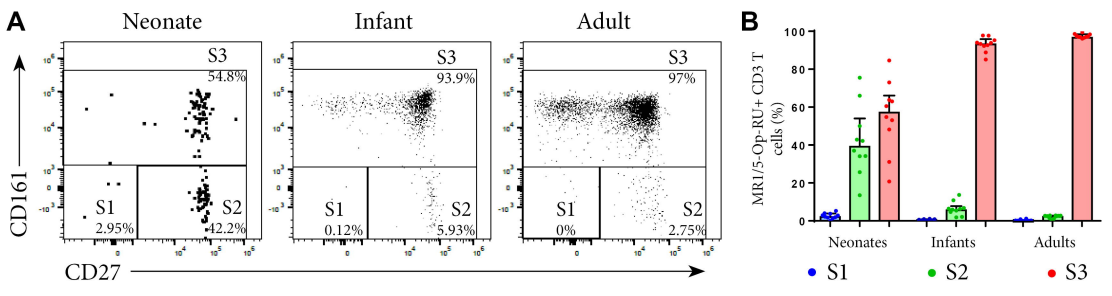
A
Neonate
Infant
Adult
S3
54.8%
S1
2.95%
S2
42.2%
S3
93.9%
S1
0.12%
S2
5.93%
S3
97%
S1
0%
S2
2.75%
CD161
CD27
B
MR1/5-Op-RU+ CD3 T cells (%)
Neonates
Infants
Adults
S1
S2
S3

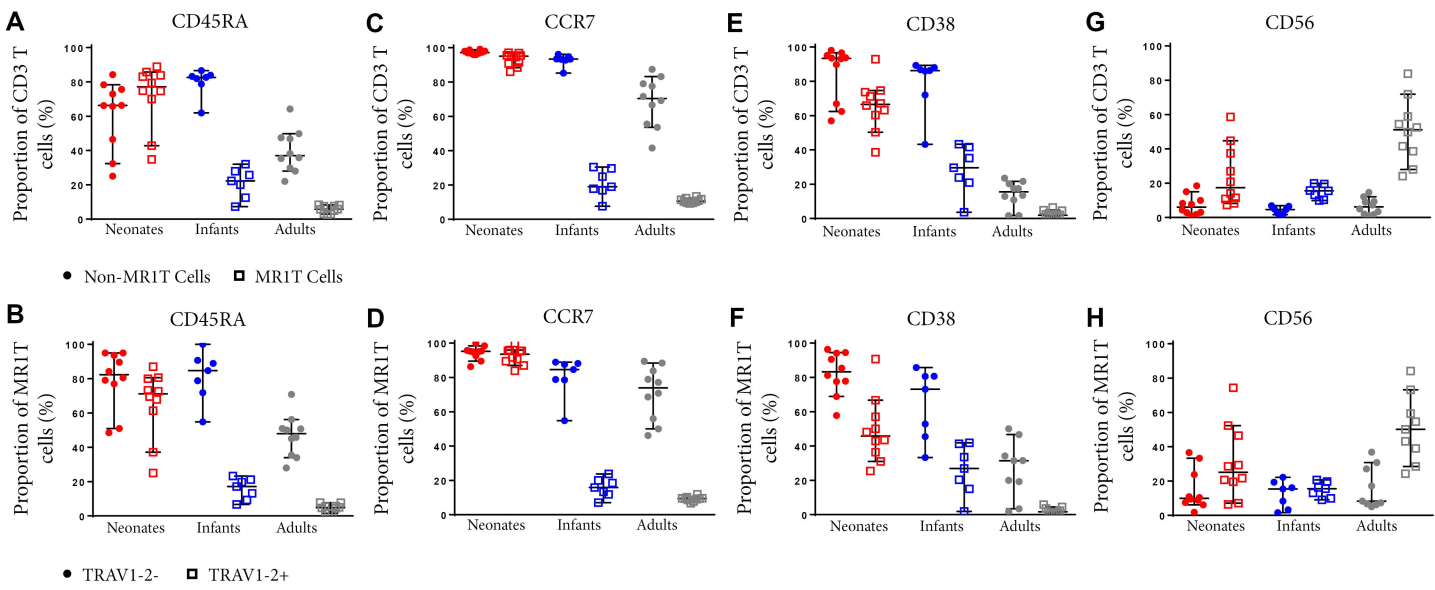
A
CD45RA
Proportion of CD3 T cells (%)
Neonates
Infants
Adults
C
CCR7
E
CD38
G
CD56
Non-MR1T Cells
MR1T Cells
B
CD45RA
Proportion of MR1T cells (%)
D
CCR7
F
CD38
H
CD56
TRAV1-2-
TRAV1-2+